AMERICAN SOCIETY FOR MICROBIOLOGY | Molecular and Cellular Biology®

RESEARCH ARTICLE

A Calcium- and Diacylglycerol-Stimulated Protein Kinase C (PKC), *Caenorhabditis elegans* PKC-2, Links Thermal Signals to Learned Behavior by Acting in Sensory Neurons and Intestinal Cells

Marianne Land, Charles S. Rubin

Department of Molecular Pharmacology, Atran Laboratories, Albert Einstein College of Medicine, Bronx, New York, USA

ABSTRACT Ca^{2+}- and diacylglycerol (DAG)-activated protein kinase C (cPKC) promotes learning and behavioral plasticity. However, knowledge of *in vivo* regulation and exact functions of cPKCs that affect behavior is limited. We show that PKC-2, a *Caenorhabditis elegans* cPKC, is essential for a complex behavior, thermotaxis. *C. elegans* memorizes a nutrient-associated cultivation temperature (T_c) and migrates along the T_c within a 17 to 25°C gradient. *pkc-2* gene disruption abrogated thermotaxis; a PKC-2 transgene, driven by endogenous *pkc-2* promoters, restored thermotaxis behavior in *pkc-2*$^{-/-}$ animals. Cell-specific manipulation of PKC-2 activity revealed that thermotaxis is controlled by cooperative PKC-2-mediated signaling in both AFD sensory neurons and intestinal cells. Cold-directed migration (cryophilic drive) precedes T_c tracking during thermotaxis. Analysis of temperature-directed behaviors elicited by persistent PKC-2 activation or inhibition in AFD (or intestine) disclosed that PKC-2 regulates initiation and duration of cryophilic drive. In AFD neurons, PKC-2 is a Ca^{2+} sensor and signal amplifier that operates downstream from cyclic GMP-gated cation channels and distal guanylate cyclases. UNC-18, which regulates neurotransmitter and neuropeptide release from synaptic vesicles, is a critical PKC-2 effector in AFD. UNC-18 variants, created by mutating Ser^{311} or Ser^{322}, disrupt thermotaxis and suppress PKC-2-dependent cryophilic migration.

KEYWORDS *C. elegans* signal integration, MUNC18 and UNC-18, calcium, diacylglycerol-activated PKC, cyclic GMP-gated channel, protein kinase C, regulation of learned behavior, sensory neuron, signal transduction, thermotaxis

Diacylglycerol (DAG) and free cytoplasmic Ca^{2+} mediate actions of hormones, neurotransmitters (NTs), and other stimuli that activate phospholipases Cβ and Cγ (1). Conventional protein kinase C isoforms (cPKCs α, βI, βII, and γ) are widely expressed effectors of Ca^{2+} and DAG in mammalian tissues (2–5). cPKCs are translocated to membranes and activated by binding Ca^{2+} and DAG via their respective C2 and C1 domains. Thus, cPKCs are poised to receive, amplify, and disseminate the complete spectrum of intracellular signals generated by phospholipase C activation. Accordingly, cPKCs often couple extracellular stimuli to physiological processes that are coregulated by dynamic changes in Ca^{2+} and DAG levels. In contrast, novel PKC isoforms (nPKCs δ, ε, η, and θ) are activated by DAG alone.

Some cell functions are redundantly regulated by combinations of PKCs. However, individual cPKCs can control key aspects of homeostasis or, when misregulated, promote pathological processes. For example, PKCα selectively regulates cardiac contrac-

Received 13 April 2017 **Returned for modification** 16 June 2017 **Accepted** 7 July 2017

Accepted manuscript posted online 17 July 2017

Citation Land M, Rubin CS. 2017. A calcium- and diacylglycerol-stimulated protein kinase C (PKC), *Caenorhabditis elegans* PKC-2, links thermal signals to learned behavior by acting in sensory neurons and intestinal cells. Mol Cell Biol 37:e00192-17. https://doi.org/10.1128/MCB.00192-17.

Address correspondence to Charles S. Rubin, charles.rubin@einstein.yu.edu.

tility, but moderate PKCα overexpression reduces cardiac contractile performance and promotes heart hypertrophy (6). Some missense mutations in PKCα, PKCβ, or PKCγ create dominant-negative kinases that enhance the progression of human cancers (7). PKCβ is an essential mediator of signal transduction in antigen-activated B cells (8). In contrast, hyperglycemia-induced activation of PKCβ promotes nephropathy and retinopathy in diabetes (9).

cPKC-mediated signaling in neurons profoundly affects learning, memory, information processing, and behavior (10–12). For instance, activated cPKCs amplify and sustain NT release that accounts for presynaptic plasticity in auditory and cerebellar synapses (13–15). In a model of auditory learning and information processing, PKCγ upregulates NT release during early development; PKCβ promotes NT release at the same synapse in mature animals. Misregulated cPKCs contribute to neurodegeneration and cognitive dysfunction. DAG binding domain mutations that reduce PKCγ catalytic activity cause spinocerebellar ataxia type 14, an autosomal dominant neurodegenerative disease (16, 17). In an Alzheimer's disease model, toxic Aβ amyloid protein disrupts synaptic structure and functions in hippocampus by promoting PKCα activation and concomitant glutamate receptor phosphorylation and endocytosis (18, 19). Supraphysiological kinase activity of PKCα variants is tightly linked to dementia in a group of families afflicted with high incidences of severe, late-onset Alzheimer's disease (18). PKCβ-deficient mice are impaired in amygdala-dependent associative learning (20). In contrast, expression of activated PKCβ in a subset of hippocampal neurons improved spatial learning in old rats, thereby counteracting age-dependent cognitive dysfunction (21).

Despite progress summarized above and related studies (10–12), knowledge of how cPKCs link sensory perception to learned behavior is constrained. Molecular and mechanistic information about upstream regulators, downstream effectors, and substrate phosphorylation sites that enable a cPKC to connect environmental stimuli to experience-dependent actions is sparse. It is desirable but challenging to discern the neurophysiological significance of cPKC-dependent signaling cascades within specific neurons, neuronal circuits, and interacting nonneuronal cells *in vivo*. Here, we address these topics by elucidating critical roles of a cPKC in regulating thermotaxis, a temperature-programmed behavior of *Caenorhabditis elegans*.

C. elegans learns and remembers a cultivation temperature (T_c) at which high-quality food is provided (22–25). When conditioned animals are exposed to a thermal gradient, thermotaxis is observed: animals migrate to the T_c and then move isothermally. Neurons comprising a thermotaxis circuit are well characterized, and thermotaxis behavior can be accurately quantified. Moreover, signaling molecules, mechanisms, and pathways employed by *C. elegans* are generally conserved in mammals. Thus, studies on a *C. elegans* cPKC can provide insights applicable to many metazoan systems.

The *pkc-2* gene encodes 6 *C. elegans* cPKCs by using three promoters and alternative splicing (26). All cPKCs share identical regulatory and kinase domains, and deletion of exons encoding these domains inactivates all PKC-2 isoforms. These prototypical cPKCs have a C-terminal kinase domain that is preceded by a pseudosubstrate site (PS), tandem DAG binding domains (C1a and C1b), and a C2 domain that ligates Ca^{2+}. Amino acid sequences of PKC-2 regulatory and kinase domains are 70 to 80% identical and $>$85% similar to domains in human cPKCs. Binding of Ca^{2+} and DAG targets PKC-2 to cell membranes and facilitates expulsion of the PS from the catalytic cleft, thereby enabling Ser/Thr phosphorylation of effector proteins (3, 5).

Here, we show that PKC-2 is indispensable for thermotaxis behavior. PKC-2 acts in both AFD sensory neurons and intestinal cells to start and sustain cold-directed (cryophilic) migration, which constitutes an early phase of thermotaxis. In AFD neurons, which control a thermotaxis circuit, PKC-2 is regulated by distal production of cyclic GMP (cGMP) via temperature-sensitive, transmembrane guanylate cyclases and the proximal influx of Ca^{2+} mediated by cGMP-gated channels. UNC-18, which regulates synaptic and dense core vesicle exocytosis, is a crucial PKC-2 effector in AFD. Candidate

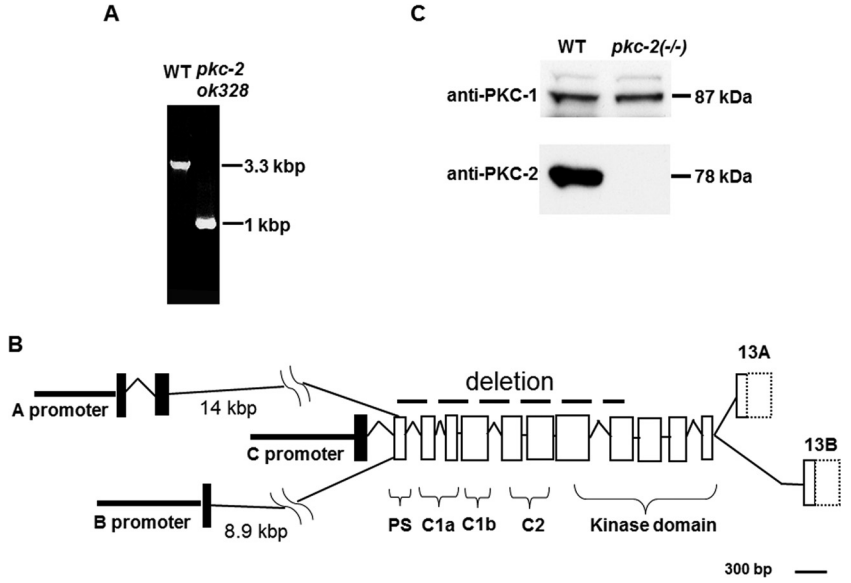

FIG 1 Gene deletion generates *pkc-2* null animals. (A) A segment of the *pkc-2* gene was amplified from DNA of WT *C. elegans* or animals carrying the *pkc-2*(*ok328*) allele. Amplified DNA was analyzed by electrophoresis in a 1% agarose gel and staining with ethidium bromide. (B) Organization of the *pkc-2* gene (26). Exons are indicated by rectangles. Exons 13A and 13B are alternatively spliced, encode unique C termini that generate PKC-2A and PKC-2B isoforms, and contain divergent 3′ untranslated sequences (dotted lines). A dashed line indicates exons and introns deleted in *pkc-2*(*ok328*) animals. Brackets identify exons that encode PKC-2 regulatory and kinase domains. (C) Proteins derived from 50 adult WT or *pkc-2*$^{-/-}$ animals were analyzed by SDS-PAGE and Western blotting (see Materials and Methods). The blot was probed with anti-PKC-2 IgGs (lower) and reprobed with anti-PKC-1 IgGs (upper). Signals were recorded on X-ray film.

PKC-2 substrate sites in UNC-18 (Ser^{311} or Ser^{322}) were mutated to Ala. Expression of either UNC-18 variant in AFD ablated PKC-2-dependent cryophilic migration and disrupted thermotaxis.

RESULTS

Characterization of a *pkc-2* deletion mutation. A *C. elegans* strain, VC127, has a homozygous deletion in a gene encoding PKC-2 (Fig. 1A). PCR amplification and sequencing revealed that 2,310 nucleotides were excised from the *pkc-2*(*ok328*) allele. The deletion begins at nucleotide 6 of exon 2 and ends at nucleotide 144 of exon 9 of *pkc-2* (Fig. 1B and reference 26). Thus, deleted exons encode the PS, C1a, C1b, and C2 regulatory domains and part of the kinase module. Three promoters (A, B, and C) (Fig. 1B) control *pkc-2* transcription (26). However, mRNAs generated from the disrupted gene will be frame shifted and contain a translation termination codon within exon 2. The small sizes of these proteins and absence of domains involved in PKC-2 regulation and catalytic activity indicate that the deletion creates a null phenotype. Hereafter, the *pkc-2*(*ok328*) allele is designated *pkc-2*$^{-/-}$.

Western immunoblotting, using IgGs directed against a segment of PKC-2 that includes amino acids 176 to 417 (26), showed that the 78-kDa PKC-2 protein was robustly expressed in wild-type (WT) animals (Fig. 1C, lower). However, PKC-2 protein was not detected in *pkc-2*$^{-/-}$ mutants. In contrast, the amount of 87-kDa PKC-1 (an nPKC internal control) was not altered by PKC-2 depletion (Fig. 1C, upper). PKC-2-deficient animals grow, develop, feed, and reproduce normally.

pkc-2 gene transcription was linked to specific cells by expressing green fluorescent protein (GFP) under the control of the A or B promoter. Robust A promoter activity was observed in AFD, AWC, ASK, and ADL sensory neurons (Fig. 2A). Strong B promoter activity was evident in intestine and muscle (Fig. 2B and C). B promoter-dependent transcription was also detected in AFD and AWC. Together, the *pkc-2* A and B promoters enrich PKC-2 mRNA expression in AFD and AWC. Partly shared properties of AFD

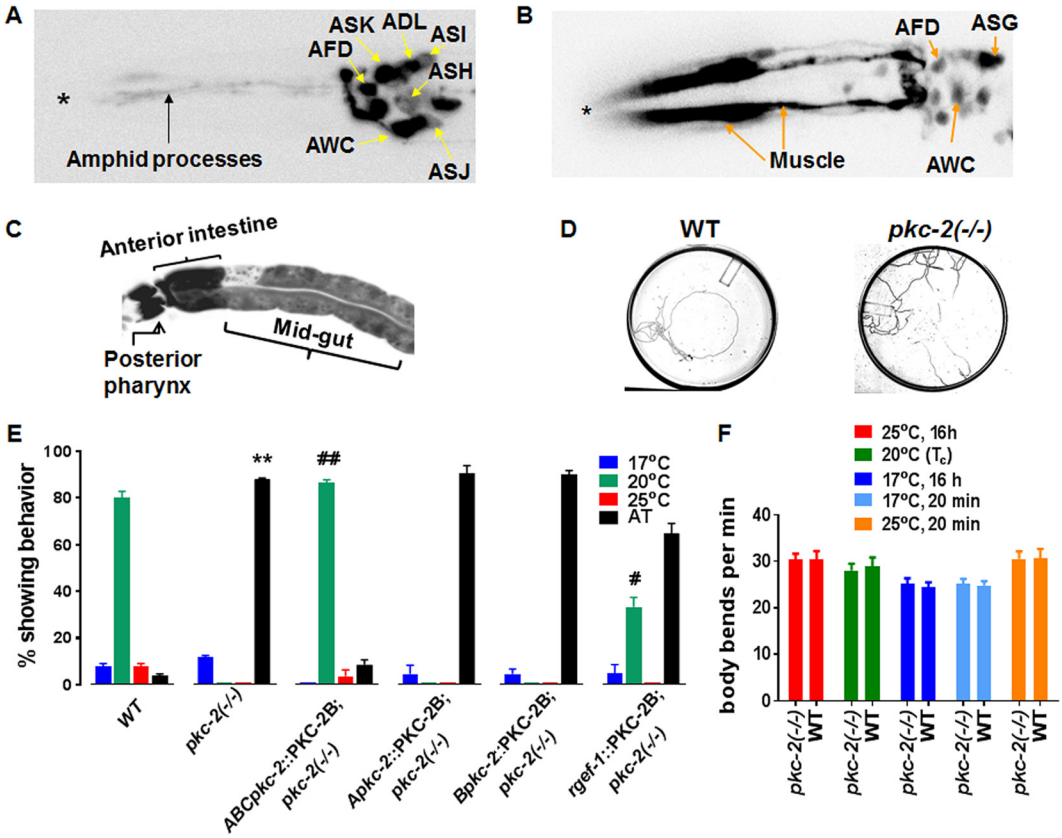

FIG 2 *pkc-2* promoters are active in sensory neurons, muscle, and intestine; PKC-2 depletion disrupts thermotaxis. (A) Neurons engaged in *pkc-2* gene transcription were identified by fluorescence microscopy of animals expressing GFP under the control of the *pkc-2* A promoter (*Apkc-2*::GFP). The micrograph extends from the head (left, asterisk) to the top of the gut (right). (B) Animals expressing a *Bpkc-2*::GFP transgene were analyzed as described for panel A. (C) Fluorescence microscopy also revealed *pkc-2* B promoter activity in pharyngeal neurons and intestine. (D) Tracks produced when WT and *pkc-2*$^{-/-}$ animals experienced a radial temperature gradient (17°C [center] to 25°C [periphery]) on a 10-cm agar plate. The T_c was 20°C. (E) WT, PKC-2-deficient, and the indicated transgenic animals were assayed for thermotaxis behavior (see Materials and Methods). Percentages of animals that migrated to the center (17°C), the T_c (20°C), or the periphery (25°C) or exhibited AT behavior were determined. Thermotaxis assays were performed with WT *C. elegans*, *pkc-2*$^{-/-}$ animals, and *pkc-2*$^{-/-}$ animals expressing PKC-2B transgenes controlled by all three *pkc-2* promoters (ABC*pkc-2*::PKC-2), the *pkc-2* A promoter, *pkc-2* B promoter, or a pan-neuronal *rgef-1* promoter (32). Results are averages obtained from three assays. Error bars are SEM. **, $P < 0.01$ compared to WT animals; ##, $P < 0.01$ compared to *pkc-2*$^{-/-}$ animals; #, $P < 0.05$ compared to *pkc-2*$^{-/-}$ animals. (F) WT and *pkc-2*$^{-/-}$ animals were assayed for locomotion on a bacterial lawn (see Materials and Methods) after brief (20 min) or prolonged (16 h) incubation at 17°C, 20°C, or 25°C. The number of body bends in a 1-min interval was determined for 10 WT or *pkc-2*$^{-/-}$ animals. Mean values and SEM are shown.

and AWC neurons suggested that PKC-2 is involved in thermotaxis. AFD directly mediates temperature perception and controls a circuit that governs thermotaxis (25, 27). AWC principally mediates responses to odorants (28). However, AWC perceives temperature and modulates thermotaxis by sending signals to the primary interneuron in the AFD-regulated circuit (29, 30). Thus, we explored the effect of PKC-2 depletion on thermotaxis.

PKC-2 deficiency compromises thermotaxis. Thermotaxis assays (see Materials and Methods) revealed that ~90% of animals lacking PKC-2 moved randomly on a 17 to 25°C gradient after cultivation at 20°C (T_c) (Fig. 2D and E). Random migration is designated atactic (AT) behavior. WT nematodes located the T_c and then tracked isothermally at 20°C (Fig. 2D and E). Thus, PKC-2 depletion caused a severe thermotaxis defect.

Thermotaxis could be compromised if PKC-2 deficiency caused movement defects. However, an established locomotion assay (31) demonstrated that PKC-2-depleted and WT animals have similar abilities for coordinated movement after brief or prolonged

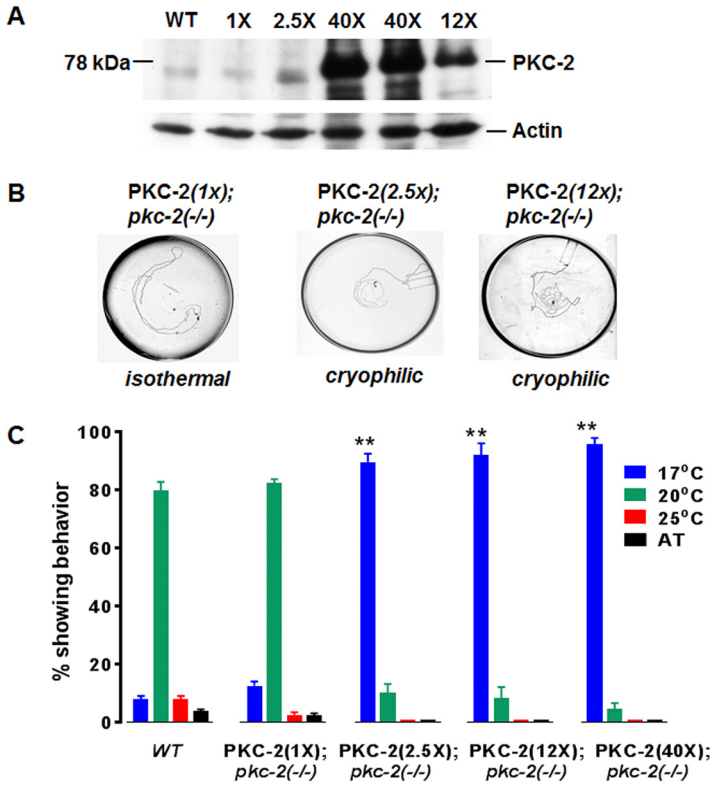

FIG 3 PKC-2 restores thermotaxis in *pkc-2* null animals; supraphysiological PKC-2 promotes cryophilic movement. (A) Proteins (30 μg) derived from WT *C. elegans* and the PKC-2(1X), PKC-2(2.5X), PKC-2(12X), and PKC-2(40X) strains described in Results were analyzed by Western immunoblotting using anti-PKC-2 IgGs as primary antibodies. ECL-based signals were generated, recorded, and quantified as described in Materials and Methods. The PKC-2 content of WT animals was taken as 1×. (B) Tracks of specified transgenic animals in thermotaxis assays. (C) Thermotaxis behavior of WT animals and transgenic strains expressing various levels of PKC-2 in the *pkc-2*$^{-/-}$ background. Assays were performed in triplicate. Mean values and SEM are shown. **, $P < 0.01$ compared to WT animals.

incubations at 17°C, 25°C, or the T_c (20°C) (Fig. 2F). Thus, PKC-2 deficiency disrupts thermotaxis, not locomotion.

PKC-2B rescues defective thermotaxis. cDNA encoding PKC-2B was cloned downstream from 3 endogenous *pkc-2* promoters (Fig. 1B) in an expression vector to create a *ABCpkc-2*::PKC-2B transgene. After microinjection into *pkc-2*$^{-/-}$ animals, strains carrying chromosomally integrated copies of the transgene were produced and characterized. Thermotaxis was fully rescued when PKC-2B expression was driven by combined actions of A, B, and C promoters (Fig. 2E). When the A or B promoter alone directed PKC-2B expression, AT behavior persisted (Fig. 2E). Similar results were obtained with the C promoter (data not shown). However, pan-neuronal expression of PKC-2B, directed by the *rgef-1* promoter (32), partly rescued thermotaxis. The proportion of animals exhibiting normal thermotaxis behavior rose from 0 to ~33% when an integrated *rgef-1*::PKC-2B transgene was expressed in all neurons of *pkc-2*$^{-/-}$ nematodes (Fig. 2E). Nevertheless, ~2/3 of the transgenic animals were AT. The results demonstrate that PKC-2 is essential for thermotaxis. Neuronal PKC-2 contributes significantly to temperature-programmed behavior. However, full restoration of thermotaxis was attained only when *pkc-2* promoters were active in both neurons and nonneuronal cells.

Elevated PKC-2 elicits cryophilic behavior. Amplified genomic DNA, which contains the 21-kbp *pkc-2* structural gene and its A, B, and C promoters, was inserted into a plasmid (*ABC*::*pkc-2*) and injected into *pkc-2*$^{-/-}$ animals. Strains carrying integrated *ABC*::*pkc*-2 DNA were produced, and PKC-2 protein abundance was normalized (relative to actin) and quantified by Western immunoblotting (Fig. 3A). Strains designated

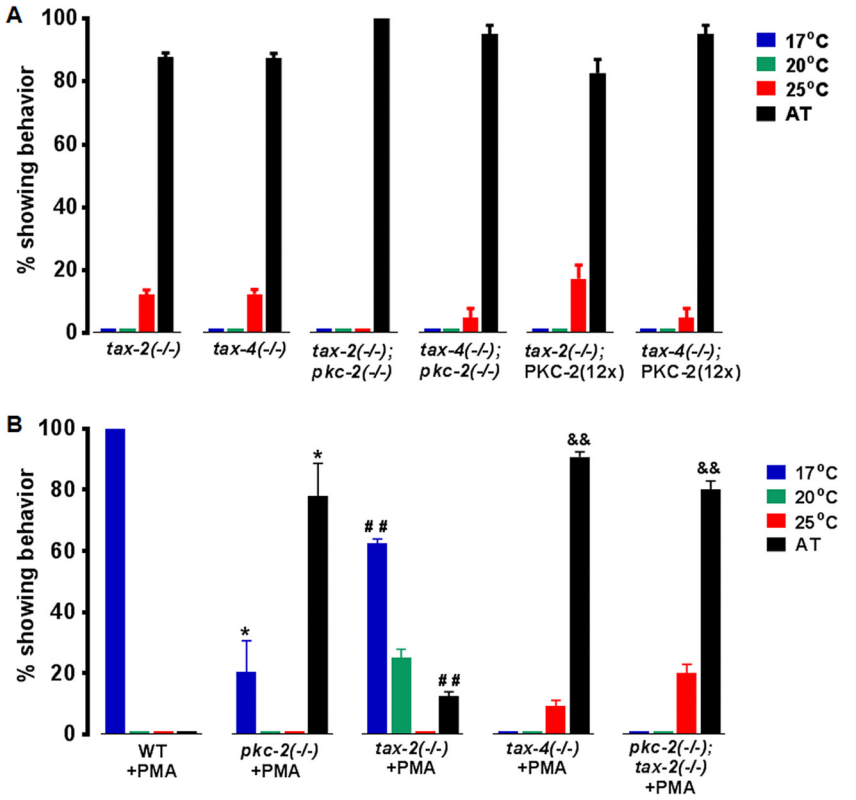

FIG 4 PKC-2 and TAX-4 are required for PMA-induced cryophilic behavior. (A) AT behavior of *tax-2* and *tax-4* null mutants is not altered by 12-fold-elevated PKC-2 or PKC-2 depletion. (B) Effects of 2 h of preincubation with 1.6 μM PMA on thermotaxis in the indicated strains. Averages from triplicate assays are presented, and error bars are SEM. *, $P < 0.05$ compared to WT animals; ##, $P < 0.01$ compared to *tax-2*$^{-/-}$ animals; &&, $P < 0.01$ compared to *tax-2*$^{-/-}$ animals treated with PMA.

PKC-2(1X), PKC-2(2.5X), PKC-2(12X), and PKC-2(40X), reflecting PKC-2 protein levels relative to WT PKC-2 content, were characterized. Thermotaxis was normal in PKC-2(1X) animals (Fig. 3B and C). In contrast, >90% of animals expressing 2.5-, 12-, or 40-fold-elevated PKC-2 migrated to the coldest point in the gradient instead of the T_c (20°C). Thus, persistently elevated PKC-2 drives cryophilic behavior.

Mutations in a cation channel suppress PKC-2-mediated cryophilic behavior. Transmembrane proteins TAX-2 and TAX-4 associate to create cGMP-gated channels in sensory neurons (33–35). TAX-4 mediates Ca^{2+} influx in AFD; TAX-2 regulates TAX-4 activity. Mutations in *tax-2* or *tax-4* disrupt thermotaxis and elicit AT behavior (Fig. 4A). Thus, we explored possible interactions between TAX-2/TAX-4 and PKC-2. Animals expressing 12-fold-elevated PKC-2 in *tax-2*$^{-/-}$ or *tax-4*$^{-/-}$ backgrounds were produced. PKC-2 overexpression did not alter AT behavior in TAX-2- or TAX-4-deficient animals (Fig. 4A). Thus, Ca^{2+} channel inactivation suppressed PKC-2-induced cryophilic behavior. Both *pkc-2*$^{-/-}$; *tax-2*$^{-/-}$ and *pkc-2*$^{-/-}$; *tax-4*$^{-/-}$ double mutants were AT. The similar phenotypes of single and double mutants indicate that PKC-2 and TAX-4/TAX-2 function in the same pathway. Although genetic analysis suggested PKC-2 acts upstream from the channel, it was equally plausible that TAX-2/TAX-4 mediates Ca^{2+} influx that is crucial for PKC-2 activation. This issue is clarified below (Fig. 4B; see also Fig. 5, 6B, and 7C).

PKC-2 mediates PMA-induced cryophilic behavior. Phorbol 12-myristate 13-acetate (PMA) mimics DAG, accumulates in membranes, avidly binds cPKCs, and is not metabolized. Thus, PMA treatment strongly enhances cPKC recruitment to membranes, thereby reducing the Ca^{2+} concentration needed for kinase activation (2). After incubation with PMA for 2 h at 20°C (T_c), WT *C. elegans* migrated to the coldest location in the temperature gradient (Fig. 4B). Thus, a PKC activator induced robust cryophilic

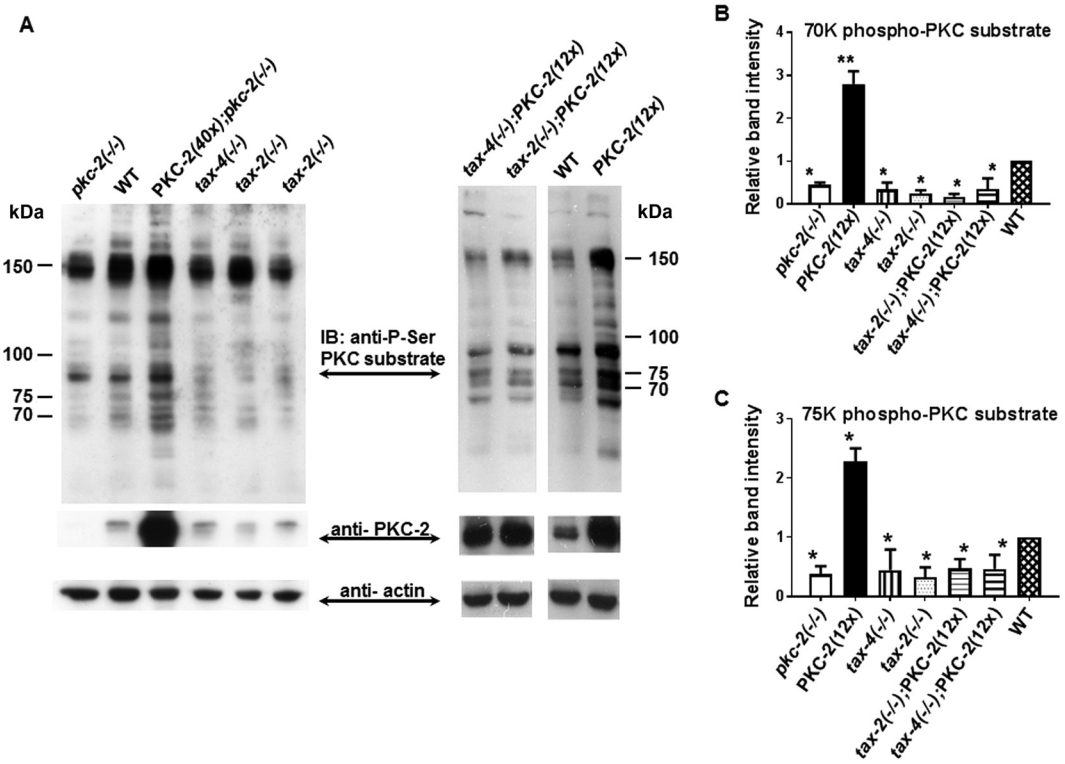

FIG 5 PKC substrate phosphorylation is diminished in *pkc-2*, *tax-2*, and *tax-4* mutants. (A) A Western blot containing samples of total protein (30 μg) from the indicated strains was prepared and probed sequentially with primary IgGs directed against phosphorylated PKC substrates, PKC-2, and actin. Signals obtained from PKC substrates were quantified and normalized to actin (see Materials and Methods). IB, immunoblot. (B and C) Abundance of phospho-p70 and phospho-p75 PKC substrates in the indicated strains. Results are averages from 3 independent experiments. Error bars are SEM. *, $P < 0.05$ compared with WT animals; **, $P < 0.01$ compared with WT animals.

behavior. However, AT behavior of *pkc-2*$^{-/-}$ animals was not affected by incubation with PMA (compare Fig. 4B to 2E). Consequently, activated endogenous PKC-2 is a critical driver of cryophilic migration.

PMA-activated PKC-2 bypasses TAX-2 depletion but not TAX-4 deficiency. When *tax-2*$^{-/-}$ *C. elegans* was treated with PMA, the number of AT animals declined 7-fold (Fig. 4B). Instead, 63% of the animals migrated to 17°C, the low point in the gradient. Thus, PMA-activated PKC-2 suppressed random movement and triggered cryophilic migration in TAX-2-deficient nematodes. PMA had no effect on AT behavior of *tax-4*$^{-/-}$ animals (Fig. 4B). The results indicate that Ca^{2+} delivered by TAX-4 alone (34, 35), in the absence of TAX-2 function, is sufficient to activate PKC-2 in concert with PMA. TAX-2, a channel modulator, cannot transmit a Ca^{2+} signal in the absence of TAX-4, which precludes PKC-2 activation. PMA-treated *pkc-2*$^{-/-}$; *tax-2*$^{-/-}$ double mutants were AT (Fig. 4B). Thus, TAX-4-mediated Ca^{2+} influx cannot elicit cryophilic migration in PKC-2-deficient animals. We conclude that PKC-2 is an essential downstream mediator of Ca^{2+}- and PMA-induced cryophilic migration. The upstream, cGMP-gated TAX-2/TAX-4 channel supplies intraneuronal Ca^{2+} that directly or indirectly promotes PKC-2 activation.

PKC-2 substrate phosphorylation is impaired by *tax-2* and *tax-4* mutations. Quantitative Western immunoblot assays, performed with an IgG that binds consensus cPKC phosphorylation sites, disclosed that substrate phosphorylation increased substantially (relative to the WT) in animals expressing elevated PKC-2 protein and decreased in *pkc-2* null nematodes (Fig. 5A, left). Affected phosphoproteins had apparent molecular mass values of 50, 63, 70, 72, 75, 85, 105, 120, 150, and 170 kDa (Fig. 5A, left). For example, phosphorylation of 70- and 75-kDa proteins (p70 and p75) increased 2.8- and 2.3-fold, respectively, in animals overexpressing PKC-2 (Fig. 5B and C). In compar-

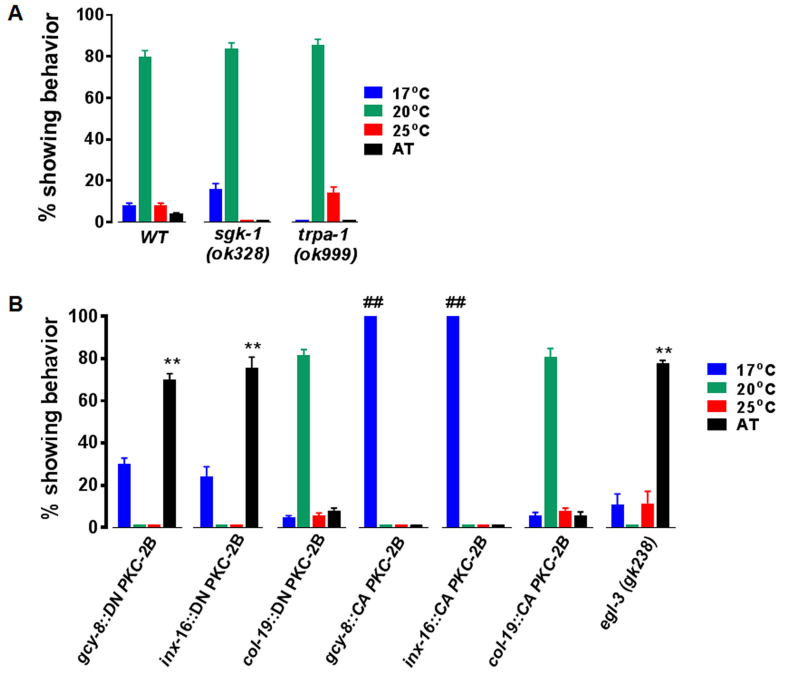

FIG 6 Thermotaxis and cryophilic behavior depend on signals transmitted by PKC-2 in AFD neurons and intestinal cells. (A) Null mutations in genes encoding TRPA-1 and SGK-1 do not affect thermotaxis. (B) DN PKC-2B and CA PKC-2B transgenes were expressed in AFD neurons (*gcy-8* promoter), intestinal cells (*inx-16* promoter), or hypodermis (*col-19* promoter) of WT animals. Thermotaxis assays were performed in triplicate as indicated in Materials and Methods; error bars are SEM. **, $P < 0.01$ compared to WT animals; ##, $P < 0.001$ compared to WT animals. Animals lacking EGL-3 have an AT phenotype.

ison with *pkc-2*$^{-/-}$ animals, elevated PKC-2 elicited 6-fold increases in p70 and p75 phosphorylation. Conversely, p70 and p75 phosphorylation decreased ~65% in animals lacking PKC-2, TAX-2, or TAX-4 (Fig. 5B and C). PKC-2 protein concentration was unchanged in TAX-2- and TAX-4-depleted animals, suggesting that diminished substrate phosphorylation was due to reduced PKC-2 kinase activity.

The TAX-2/TAX-4 channel was essential for robust substrate phosphorylation associated with PKC-2 overexpression (Fig. 5A, upper right). Despite a 12-fold augmentation in PKC-2 content, substrate phosphorylation was reduced 70 to 90% by TAX-2 or TAX-4 depletion (Fig. 5B and C). Thus, Ca^{2+} entry through upstream TAX-2/TAX-4 channels is critical for PKC-2 activation and, hence, downstream signal transmission underlying thermotaxis behavior.

***pkc-2* gene promoters are active in neurons that express TAX-2 and TAX-4.** TAX-2 and TAX-4 are expressed in 20 neurons that mediate chemosensation, thermal sensation, nociception, and aerotaxis (33, 34, 36). PKC-2 is coexpressed with TAX-2 and TAX-4 in a subset of these sensory neurons, including AFD (Fig. 2A). Thus, PKC-2 activation by TAX-2/TAX-4-mediated Ca^{2+} influx is restricted to sensory neurons.

The TRPA-1 cation channel is dispensable for PKC-2-mediated thermotaxis. TRPA-1, a cation ion channel, mediates Ca^{2+} influx in intestinal cells when *C. elegans* encounters low temperature (≤20°C) (37). Signals carried by Ca^{2+} are transmitted to the nucleus by a cascade composed of PKC-2, serum-glucocorticoid activated kinase 1 (SGK-1), and DAF-16, a transcription factor. Activated DAF-16 orchestrates gene expression that alleviates stress and extends *C. elegans* life span at low temperature. These observations suggested that TRPA-1-dependent Ca^{2+} influx might promote thermotaxis by activating intestinal PKC-2, and SGK-1, a PKC-2 effector, might disseminate downstream signals underlying thermotaxis. However, thermotaxis was not impaired in animals carrying *trpa-1* or *sgk-1* null mutations (Fig. 6A). PKC-2-dependent thermotaxis is not regulated by TRPA-1 or mediated by SGK-1.

Thermotaxis is codependent on actions of PKC-2 in AFD neurons and intestine. AFD neurons are the principal thermosensory cells of the *C. elegans* nervous system (25). In AFD, temperature-regulated guanylate cyclases (GCYs) catalyze synthesis of cGMP (38), which binds and allosterically activates TAX-2/TAX-4 channels. Thermal signals are ultimately transmitted to interneurons (for processing and integration) and associated motor neurons that guide migration and isothermal tracking behavior (25). Robust PKC-2 expression in TAX-2/TAX-4-enriched AFD neurons suggested PKC-2 coupled Ca^{2+} signals to regulation of the thermosensory circuit by promoting NT and/or neuropeptide (NP) release from AFD.

We explored this idea and also investigated the role of nonneuronal PKC-2 in thermal signaling by determining how targeted PKC-2 activation/inactivation in AFD or nonneuronal cells impacted behavior. Validated mutations were introduced into PKC-2B to create dominant-negative (DN) or constitutively active (CA) variants (39–42). Replacement of Lys^{376} with Arg ablates ATP binding at the catalytic site of DN PKC-2B. Replacement of Ala^{27} with phosphomimetic Glu excludes the pseudosubstrate segment of PKC-2B from the protein substrate binding site, thereby creating a CA kinase. We used cell-specific *gcy-8*, *inx-16*, or *col-19* gene promoters to target transcription of DN or CA PKC-2B transgenes to AFD neurons (43), intestinal cells (44), or hypodermal cells (45), respectively.

Expression of DN PKC-2B in AFD disrupted thermotaxis (Fig. 6B). No animals migrated to the T_c and approximately 70% were AT. Expression of DN PKC-2B in intestinal cells also extinguished thermotaxis and caused AT movement in ~75% of transgenic animals. Thus, inhibition of PKC-2-dependent signaling in either AFD neurons or intestine elicited behavior that resembles the AT phenotype of *pkc-2* null nematodes (Fig. 2E), which lack PKC-2 in intestine, muscle, and many neurons (26). In contrast, ~80% of animals expressing DN PKC-2B in hypodermal cells migrated to the T_c (Fig. 6B). This parallels WT thermotaxis behavior (Fig. 2E and 6A). Thus, inhibitory effects of DN PKC2B are cell specific and not due to transgene expression *per se*. PKC-2 activation in AFD is essential but not sufficient for temperature-programmed behavior. Activation of PKC-2 in intestinal epithelial cells is also indispensable but insufficient for thermotaxis. Thermotaxis behavior is evidently learned and remembered by integrating mutually interdependent signals emanating from AFD neurons and intestinal cells.

Impaired neuro- and endocrine peptide processing disrupts thermotaxis. The AFD circuit and intestine may communicate by secreting NPs and endocrine peptides from dense core vesicles (DCVs). Therefore, we assessed thermotaxis in animals homozygous for a null allele of *egl-3*, which encodes the major proprotein convertase in *C. elegans* (46). EGL-3 endoprotease depletion severely diminishes conversion of inactive precursors into bioactive neuro- and endocrine peptides. Nearly 80% of animals lacking EGL-3 were AT (Fig. 6B). Thus, impaired NP and endocrine peptide biogenesis and suppression of PKC-2 activity in AFD or intestinal cells yielded similar phenotypes. Further analysis is needed, but the data raise the possibility that PKC-2 regulates gut-neuron cross talk during thermotaxis by promoting peptide secretion.

Sustained PKC-2 activation in AFD or intestine causes cryophilic behavior. Accumulation of CA PKC-2 in either AFD or intestinal cells elicited robust cryophilic behavior (Fig. 6B). The phenotype mirrors cold-directed migration induced by 2.5- to 40-fold elevation of PKC-2 in multiple neurons, intestinal cells, and muscle (Fig. 3C). Thermotaxis was normal when CA PKC-2 was targeted to hypodermis. Thus, PKC-2 effectors in AFD and intestinal cells shape *C. elegans*' responses to thermal signals by promoting cryophilic migration. Transient, cold-directed movement constitutes an initial phase of thermotaxis (23, 47). Persistent cryophilic behavior induced by CA PKC-2 implies that cell-specific inactivation of PKC-2 and PKC-2 effectors is a prerequisite for transition to the terminal phase of thermotaxis, isothermal tracking at the T_c. Thermotaxis is evidently governed by integrating input signals derived from intestine and the AFD circuit. Inputs must be maintained within a precise range, because excessive or diminished PKC-2-dependent signaling in AFD or intestine sufficiently distorts the integrated signal to preclude thermotaxis and generate cryophilic or AT behavior.

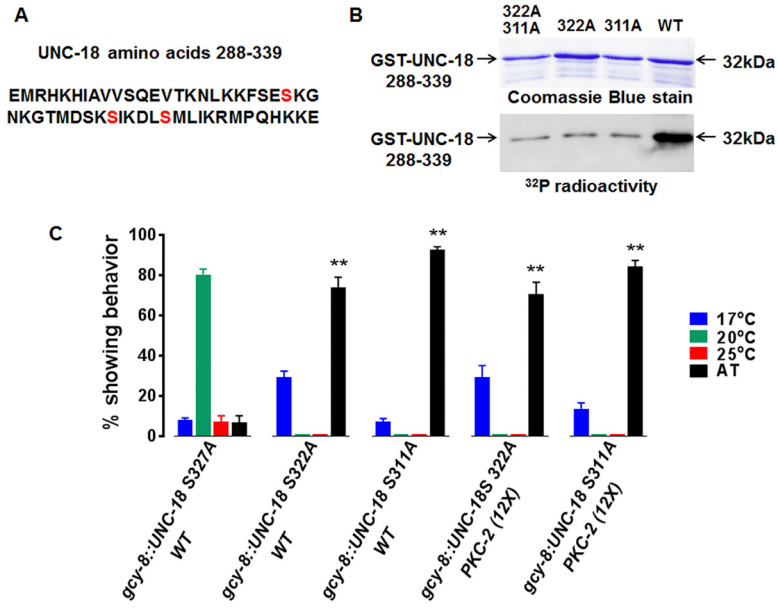

FIG 7 UNC-18 is an essential PKC-2 effector in AFD neurons. (A) Sequence of amino acids 288 to 339 in UNC-18. Potential PKC-2 substrate sites are marked in red. (B) Samples (1 μg) of affinity-purified, WT, or mutant GST–UNC-18 288-339 fusion proteins were incubated with Mg-[γ-^{32}P]ATP and activated PKC-2B T651E as described in Materials and Methods. Fusion protein phosphorylation was analyzed by SDS-PAGE (15% gel) and autoradiography as described previously (80). (Upper) Fusion proteins stained with Coomassie blue. Proteolytic fragments that retain the GST tag are evident below intact fusion protein. (Lower) Corresponding autoradiogram. (C) Ala was substituted for Ser^{311} or Ser^{322} in full-length UNC-18. Expression of either mutant in AFD abrogated thermotaxis in WT animals and blocked cryophilic migration induced by 12× PKC-2B overexpression. Expression of UNC-18 S327A in AFD did not alter thermotaxis. Assays were performed in triplicate; error bars are SEM. **, $P < 0.01$ compared to WT animals.

UNC-18, a PKC-2 effector, is essential for thermotaxis. Mammalian Munc18 and the *C. elegans* homolog UNC-18 mediate signal-regulated NT and NP secretion by interacting with SNARE proteins and promoting the docking, priming, and exocytosis of synaptic vesicles (SVs) and DCVs (48–51). In the calyx of Held auditory synapse, cPKCs transmit Ca^{2+} and DAG signals by phosphorylating Ser or Thr in the 3a domain of Munc18 (13, 52–56). Phospho-Munc18 upregulates NT release by enhancing SV exocytosis.

Phosphorylation site identification software (NetPhos3.1 and GPS3.0) and previous studies (53, 55) indicated that a predicted loop in the UNC-18 3a domain contains candidate PKC-2 substrate sites: serines 311, 322, and 327 (Fig. 7A). cDNA encoding an UNC-18 fragment (amino acids 288 to 339) was cloned downstream from a glutathione *S*-transferase (GST) gene in an expression plasmid. In separate constructs, relevant serines were mutated to Ala. WT and mutated versions of 32-kDa GST–UNC-18 288-339 fusion proteins were expressed in *Escherichia coli* and purified by affinity chromatography (Fig. 7B). CA PKC-2B T651E robustly phosphorylated WT fusion protein. Unmodified GST was not phosphorylated (not shown). Replacement of either Ser^{322} or Ser^{311} with Ala suppressed PKC-2B-catalyzed phosphorylation by ~90%. Thus, PKC-2B catalyzes highly cooperative, *in vitro* phosphorylation of Ser^{311} and Ser^{322} in the recombinant UNC-18 3a domain. Functions of Ser^{311} and Ser^{322} were assessed by *in vivo* analysis.

Replacement of PKC substrate sites in Munc18 with Ala creates DN proteins that inhibit Ca^{2+}- and DAG-dependent enhancement of SV or DCV exocytosis in stimulated neurons (54, 56–58). Therefore, mutations described above were introduced into cDNA encoding full-length UNC-18. The physiological relevance of Ser^{311} and Ser^{322} was examined by expressing mutant UNC-18 transgenes in AFD neurons. Thermotaxis was normal in animals expressing UNC-18 Ala^{327} (Fig. 7C). However, substitution of Ala for

Ser^{311} or Ser^{322} generated DN UNC-18 proteins that abrogated thermotaxis in a WT background. Populations of animals expressing UNC-18 Ala^{311} or UNC-18 Ala^{322} in AFD neurons were 74% and 92% AT, respectively (Fig. 7C). Thus, both Ser^{311} and Ser^{322} in UNC-18 are essential for coupling upstream thermal, cGMP, and Ca^{2+} signals to regulation of NT and/or NP release at AFD axons.

Accumulation of DN UNC-18 Ala^{322} or Ala^{311} in AFD neurons suppressed cryophilic migration in animals containing 12-fold-elevated PKC-2B and triggered AT behavior in >70% of the population (Fig. 7C). Thus, UNC-18 is a PKC-2B effector. The results raise the possibility that diphosphorylation of UNC-18 is required for temperature-programmed behavior. Overall, GCY- and TAX-2/TAX-4-induced increases in cGMP and Ca^{2+} in AFD are linked to enhanced synaptic transmission by a PKC-2/UNC-18 signaling module which promotes NT and/or NP release.

DISCUSSION

A null mutation in the *C. elegans pkc-2* gene extinguished thermotaxis, a learned behavior, and caused AT movement in a thermal gradient. Thermotaxis was fully restored by using authentic *pkc-2* promoters to direct expression of a physiological level of PKC-2B in *pkc-2*$^{-/-}$ animals. Thus, PKC-2 is critical and indispensable for linking thermosensory signals to experience-dependent behavior.

A modest partial rescue of thermotaxis, achieved when a pan-neuronal promoter directed PKC-2B expression in *pkc-2*$^{-/-}$ animals (Fig. 2E), raised an unanticipated but important question. Is thermotaxis dependent on nonneuronal cells acting in concert with the AFD-controlled neuronal circuit? DN PKC-2B or CA PKC-2B proteins were targeted to specific cells to address this question. DN inhibition of PKC-2 in either AFD neurons or intestinal cells elicited strong AT behavior, thereby replicating a *pkc-2* null phenotype in a WT background. When CA PKC-2B accumulated in AFD or intestinal cells, elevated kinase activity elicited profound cryophilic behavior in the WT background. Similar cryophilic behavior occurred when *ABC*::PKC-2B transgenes directed 2.5- to 40-fold PKC-2 overexpression in *pkc-2*$^{-/-}$ animals. Thus, thermotaxis progresses normally only when cooperating PKC-2-dependent signaling pathways operate in both AFD neurons and intestinal cells. Further, PKC-2 acts within a limited physiological range of concentration and activity. Both diminished and elevated PKC-2 abrogate thermotaxis and promote strongly penetrant, alternate behaviors.

Activated PKC-2 switches on cryophilic drive, the first phase of thermotaxis (see Materials and Methods and reference 47). However, persistently increased PKC-2 activity overrides the transition to T_c tracking and supports sustained, cold-directed migration. To establish isothermal tracking behavior, PKC-2 activity must be suppressed as animals reach the T_c. This implies that signal (temperature?)-dependent protein phosphatases, which inactivate PKC-2 and PKC-2 effectors, also play a decisive role in thermotaxis.

How could PKC-2-mediated signaling pathways in AFD neurons and gut cooperate to shape thermotaxis? PKC-2 may promote neuron-gut cross talk by upregulating NP and/or endocrine peptide secretion. Mutational inactivation of EGL-3, an endoprotease that mediates NP processing in AFD (46), caused AT behavior that parallels random migration induced by PKC-2 depletion. Moreover, a major function of UNC-18, a PKC-2 effector, is to accelerate NT and NP release from SVs and DCVs in axons (48–51). PKC-2-mediated activation of UNC-18 in AFD could stimulate *trans*-synaptic release of NT to interneurons and also promote secretion of a diffusible NP from DCVs to send thermal signals to intestine. We speculate that temperature-regulated, PKC-2-mediated secretion of endocrine peptides from intestinal cells could trigger receptor-mediated variations in Ca^{2+} and DAG in AFD, thereby modulating PKC-2 activity and UNC-18 phosphorylation. Inputs received from AFD and intestine appear to be integrated to yield a unified output signal that regulates initiation and duration of the cryophilic phase of thermotaxis. Future studies are needed to (i) determine if impaired endocrine peptide processing in intestine compromises thermotaxis, (ii) identify peptides, receptors, and pathways that mediate neuron-gut interactions relevant to thermotaxis, and

(iii) demonstrate PKC-2 regulates secretion of relevant neuro- and endocrine peptides from AFD and intestinal cells.

Thermotaxis begins when temperature-sensitive GCYs produce cGMP in the AFD dendrite (38). cGMP binds and activates TAX-2/TAX-4, which mediates Ca^{2+} influx and depolarization (25, 33–35). Elevated Ca^{2+} modulates thermotaxis by upregulating Ca^{2+}/calmodulin-activated protein kinase 1 (CMK-1) or calcineurin (TAX-6), a protein phosphatase. CMK-1 induces *gcy* gene expression, whereas TAX-6 is required to sustain optimal TAX-2/TAX-4-mediated Ca^{2+} uptake (59, 60). Neither CMK-1 nor TAX-6 directly regulates NT or NP release from vesicles. Thus, signaling in AFD that connects TAX-2/TAX-4 activation to temperature-programmed behavior is not fully understood.

To address this problem we elucidated contributions of PKC-2 activity, PKC-2 regulatory domains, and a PKC-2 effector to thermotaxis. PMA, a PKC activator, induced cryophilic behavior in WT *C. elegans* but not in *pkc-2*$^{-/-}$ animals. Endogenous, Ca^{2+}-independent, DAG/PMA-activated nPKCs (PKC-1 and TPA-1), which are expressed in AFD neurons and intestine, did not compensate for PKC-2 depletion. Moreover, activation of a normal physiological amount of PKC-2 was sufficient to trigger cold-directed migration. Thus, PKC-2 is a unique and essential cryophilic effector of PMA.

TAX-2- and TAX-4-deficient animals are AT. PMA elicited strong cryophilic migration in TAX-2-depleted animals but did not alter AT behavior caused by TAX-4 deficiency. High DAG or PMA concentrations markedly decrease Ca^{2+} levels required for kinase activation (2). PMA-activated PKC-2 bypassed mutational inactivation of the TAX-2 regulatory protein because TAX-4 self-associates to generate functional channels (34). In concert with abundant PMA, homo-oligomeric TAX-4 channels supply sufficient Ca^{2+} for translocation and activation of PKC-2. Thus, PKC-2 acts downstream from the cation channel and Ca^{2+} in the thermotaxis signaling pathway. The data also show that DAG/PMA-binding C1 domains of PKC-2 play a crucial role in mediating the cryophilic phase of thermotaxis. In *tax-4*$^{-/-}$ animals, the cation carrier is absent, cGMP-gated Ca^{2+} influx is extinguished, and, hence, PKC-2 is not activated. In the absence of elevated PMA or DAG, TAX-2 or TAX-4 deficiency blocked cryophilic behavior in animals expressing 12-fold-elevated PKC-2. These data confirm that PKC-2 is a Ca^{2+} sensor and signal amplifier (via C2 and kinase domains) that operates downstream from proximal cGMP-gated channels and distal GCYs.

Remarkably, similar phenotypes caused by increasing WT PKC-2 concentration in many cells, incubating WT or *tax-2*$^{-/-}$ animals with PMA, or expressing CA PKC-2B only in AFD neurons or gut indicate that phosphorylation of PKC-2 effectors in AFD or intestinal cells is sufficient to trigger cryophilic behavior.

Mammalian MUNC18 and homologous *C. elegans* UNC-18 interact with SNARE protein complexes to regulate docking, priming, and exocytosis of SVs and DCVs (50, 51, 57, 58, 61–63). Repetitive electrical stimulation of murine auditory and cerebellar synapses substantially raises the rate of NT release (15, 54). Increased exocytosis persists for a long interval after stimulation is terminated. This important form of presynaptic plasticity is controlled by cPKC-mediated, multisite phosphorylation of MUNC18 (54, 56–58). *C. elegans* reduces its rate of locomotory muscle contractions by ~65% immediately after transfer to a noxious, supraphysiological temperature (28°C). Neurotransmission underlying temperature-dependent inhibition of locomotion was compromised in *pkc-2*$^{-/-}$ animals (55). A DN UNC-18 protein was generated by mutating Ser^{311}, a PKC-2 substrate site, to Ala. Expression of DN UNC-18 in AFD (WT background) replicated the locomotion defect observed in PKC-2-deficient animals. The results suggest that phospho-UNC-18 mediates temperature-dependent suppression of muscle contraction. The studies on mammalian and *C. elegans* neurons revealed that UNC-18 has the requisite functional and regulatory properties to serve as a PKC-2 effector in a signaling pathway that controls thermotaxis.

Previous work on UNC-18 and PKC-2 in AFD neurons was limited in scope (muscle contraction) and signal transduction analysis (55). The ability of PKC-2 to phosphorylate Ser^{311} in UNC-18 was not directly demonstrated. Only one of several potential PKC-2 regulatory sites in UNC-18 was characterized. Upstream regulators of PKC-2 and UNC-18

were not identified. Importantly, roles of PKC-2 and UNC-18 in experience-dependent thermotaxis behavior were not investigated.

We show that PKC-2 phosphorylates GST–UNC-18 288-339 at Ser^{311} and Ser^{322} in a highly cooperative manner. Mutation of either Ser^{311} or Ser^{322} to Ala generated DN UNC-18 variants. Expression of UNC-18 Ala^{311} or UNC-18 Ala^{322} in AFD neurons had no impact on locomotion but instead abolished thermotaxis and caused AT migration in a thermal gradient. Accumulation of DN UNC-18 in AFD also suppressed cryophilic behavior in animals expressing 12-fold-elevated PKC-2. Thus, UNC-18 is a critical PKC-2 effector. The data suggest that PKC-2-catalyzed phosphorylation of both Ser^{311} and Ser^{322} is essential for activating UNC-18 effector functions. Activated UNC-18 will promote *trans*-synaptic release of NT or NP, thereby transmitting thermal signals from AFD to receptors on downstream neurons in a circuit that guides thermotaxis. A homology-based model places serines 311 and 322 in a loop that links two antiparallel α-helices in the UNC-18 3a domain (55). Structures determined for homologous MUNC18 and its binding partners revealed that segments of the α-helix adjoining the C terminus of the specified loop mediate interactions with v- and t-SNARE complexes and syntaxin (61–63). This suggests that Ser^{311} and Ser^{322} are well positioned to participate in the reversible regulation of UNC-18 functions via phosphorylation and dephosphorylation.

Caution must be exercised before endorsing the preceding, plausible explanation of PKC-2 action in AFD neurons. Currently, we lack direct evidence documenting UNC-18 phosphorylation *in vivo*. Future development and application of phosphospecific antibodies that detect and discriminate among UNC-18 P-Ser^{311}, UNC-18 P-Ser^{322}, and diphosphorylated UNC-18 P-Ser^{311}, P-Ser^{322} can address this limitation and enable verification or refutation of the proposed mode of PKC-2 action.

Our conclusions converge with two emerging concepts. First, *C. elegans* intestine is a key locus of temperature perception, and second, neuron-gut interactions play critical roles in processing thermosensory signals that regulate physiology and behavior. AFD neurons transmit signals that sustain a normal life span at warmer temperatures (25°C). Elevated temperature elicits CMK-1-dependent *flp-6* gene expression in AFD (64). FLP-6, an FMRFamide family peptide, is released as an NT at the AFD-AIY interneuron synapse, thereby regulating thermosensory circuitry. In parallel, FLP-6 is secreted as a diffusible NP from DCVs in AFD. Acting via receptors on intestinal and other cells, FLP-6 suppresses INS-7 secretion from intestine and promotes DAF-16-mediated transcription. Together, decreased INS-7 and activated DAF-16 upregulate expression of stress genes that protect against temperature-induced toxicity. In future studies, INS-7 and FLP-6 merit consideration as candidate mediators of AFD-intestine interactions underlying thermotaxis.

C. elegans life span at lower temperatures ($<$20°C) is sustained by activation of TRPA-1, a cold-sensitive Ca^{2+} channel (37). PKC-2 serves as the Ca^{2+} sensor. SGK-1, a PKC-2 effector, phosphorylates nuclear DAF-16, which upregulates transcription of cold stress response genes that optimize life span at low temperature. Genetic and physiological analyses further demonstrated that intestinal cells are intrinsically cold sensitive. The TRPA-1–PKC-2–SGK-1 cascade is not involved in thermotaxis, as documented in Fig. 6A and associated text in Results.

TAX-2 and TAX-4 are not expressed in intestine and TRPA-1 is not required for thermotaxis. Consequently, a channel or transporter that supplies intestinal free Ca^{2+} to activate PKC-2 during the cryophilic phase of thermotaxis remains to be identified. UNC-18 has not been detected in intestine, and SGK-1, an established PKC-2 effector, is not required for thermotaxis. Thus, the intestinal contribution to thermotaxis must be shaped by distinct PKC-2 substrates. The *C. elegans* genome encodes a putative MUNC18 family protein (designated T07A9.10 in the WormBase database) that is 35% identical and 59% similar to neuronal UNC-18 and contains predicted PKC-2 phosphorylation sites. If future analysis reveals that the UNC-18 homolog accumulates in intestine, it will be investigated as a candidate PKC-2 effector that may regulate secretion of endocrine peptides that bind receptors in the AFD circuit.

DAG-activated PKC-1, a PKCε homolog, is essential for thermotaxis (65). However, PKC-1-deficient *C. elegans* migrates to the maximum temperature in a thermal gradient. Normal thermotaxis is restored in *pkc-1*$^{-/-}$ animals by expressing PKC-1 only in AFD neurons. Moreover, PKC-1 has not been implicated in thermosensory signaling in nonneuronal cells or in mediating the exchange of signals between neurons and intestine. PKC-1 does not substitute for PKC-2, but its exact function is not known. Thermotaxis is not affected by mutations in TPA-1, a distinct, DAG-activated PKCδ homolog. However, in a striking precedent, studies on Na^+-dependent chemotaxis revealed that TPA-1 is required for behavioral plasticity and integrative transmission of signals between the nervous system and intestine (66). Activation of DAG-controlled TPA-1 in both a neuronal circuit and intestinal cells and communication between intestine and neurons are essential for associative learning underlying an experience-dependent switch from Na^+ attraction to Na^+ aversion.

C. elegans adapts to increases in T_c by memorizing a new T_c within 2 h. Animals lacking HSF-1, a heat shock transcription factor, cannot adapt and exhibit cryophilic behavior (67). Targeted expression of HSF-1 in muscle or intestine of *hsf-1*$^{-/-}$ animals promotes estradiol synthesis. Binding of estradiol by receptors in AFD, AWC, and AIY neurons generates signals that restore adaptation in the *hsf-1*$^{-/-}$ background. The relevance of PKC-2 to T_c adaptation or HSF-1 action is unknown, but *hsf-1* and *pkc-2* mutants have distinct phenotypes. Moreover, expression of HSF-1 in several neurons rescues the *hsf-1* null phenotype while bypassing nonneuronal cells. Nevertheless, the discovery of HSF-1-dependent adaptation demonstrates that *C. elegans* can deploy endocrine mechanisms to integrate thermal signals acquired by intestine with neuronal inputs to modify behavior.

Overall, current results suggest a working model: thermal signals carried by cGMP and Ca^{2+} are received by PKC-2 in AFD. Ca^{2+}-activated PKC-2 amplifies and targets signals to docked secretory vesicles by activating its effector, UNC-18. Activated UNC-18 promotes exocytosis of NTs from SVs, thereby upregulating synaptic transmission to the AIY interneuron and enhancing the information-processing, signal-integrating, and motor output activities of the AFD-controlled circuit. In principle, activated UNC-18 could also trigger release of NPs from DCVs in AFD. A diffusible NP could mediate positive or negative cross talk by relaying signals to receptors on distal, nonneuronal cells, such as intestinal epithelial cells. In parallel, temperature-dependent activation of PKC-2 in intestine may promote secretion of endocrine peptides that bind with receptors in AFD or downstream neurons in the AFD circuit. This would enable integration of nonneuronal and neuronal signals to qualitatively and quantitatively shape thermotaxis behavior.

MATERIALS AND METHODS

***C. elegans* growth and strains.** *C. elegans* was grown and maintained at 20°C as previously described (68). PR691 *tax-2*(*p691*), PR671 *tax-2*(*p671*), PR678 *tax-4*(*p678*), VC461 *egl-3*(*gk238*), TQ1516 *trpa-1*(*ok999*), and VC345 *sgk-1*(*ok538*) strains were obtained from the *C. elegans* Genetics Center (CGC; University of Minnesota, Minneapolis, MN). VC127 *pkc-2*(*ok328*) was acquired from the *C. elegans* Gene Knockout Consortium (University of British Columbia, Vancouver, BC, Canada). VC127 was backcrossed into the WT (N2) genetic background 7 times. Double-mutant strains were constructed using standard genetic methods and verified by complementation and/or sequencing relevant PCR-amplified DNA fragments.

Genomic DNA amplification. Segments of the *pkc-2* gene were amplified by PCR as previously described (32, 69). Samples of genomic DNA prepared from WT animals or mutant animals homozygous for a *pkc-2* gene deletion [*pkc-2*(*ok328*) allele] were used as PCR templates. Two rounds of PCR were performed using nested primers. External and internal left primers were 5′-GCTGAAAAGGCTTCACGAA-3′ and 5′-ACCTCCCAATTTGCTTCCTT-3′, respectively. External and internal right primers were 5′-CCGGAG TTCCACAGAATGT-3′ and 5′-CGTCTCGTTCGAGCATAAC-3′, respectively. DNA sequencing was used to characterize amplified *pkc-2* gene fragments and determine the 5′ and 3′ boundaries of the gene deletion.

Preparation and electrophoresis of *C. elegans* proteins. Larval stage 4 animals were suspended in 30 mM Tris-HCl buffer (pH 8.5) containing 7 M urea, 2 M thiourea, 4% 3-[(3-cholamidopropyl)-dimethylammonio]-1-propanesulfonate (CHAPS), 1.5 mg/ml dithiothreitol (DTT), 2 μg/ml pepstatin A, and 20 μM 4-amidinophenylmethanesulfonyl fluoride hydrochloride and frozen dropwise in liquid nitrogen. The frozen animals were pulverized in a liquid nitrogen-cooled pestle, thawed, and further

disrupted by using a French press at 1,200 lb/in^2. The lysate was clarified by centrifugation at 16,000 × *g* for 20 min at 4°C. Gel loading buffer was added and proteins were size-fractionated by SDS-PAGE as previously described (70).

Protein determination. Protein concentrations were determined with the Bio-Rad DC protein assay. Bovine albumin was employed as a standard.

Electrophoresis of proteins and Western immunoblot assays. Proteins were separated by electrophoresis in a denaturing polyacrylamide gel (70). Precision Plus Protein polypeptides (Bio-Rad) were used as molecular size markers. Western blots of fractionated proteins were prepared and incubated with primary IgGs as previously reported (68, 71). Lanes in Western blots received 30 μg of protein. Antigen-antibody complexes were visualized and quantified by using peroxidase-coupled secondary IgGs in combination with chemiluminescence reagents and image analysis software (ImageQuant, GE Healthcare). Signals were recorded on X-ray film.

Antibodies. Affinity-purified IgGs that bind PKC-1 and PKC-2 were produced as previously described (26, 68). Anti-actin IgG was obtained from Biomedical Technologies (Stoughton, Massachusetts). An antibody that binds consensus PKC phosphorylation sites, R/K-X-S(P)-Φ-R/K [where Φ is a hydrophobic amino acid, S(P) is phosphoserine, and X is any amino acid], was obtained from Cell Signaling Technology. All primary antibodies were produced in rabbits. Horseradish peroxidase-coupled secondary IgG (Amersham) was purchased from GE Healthcare Biosciences (Pittsburgh, PA).

Locomotion assay. Locomotion was monitored and quantified as described by Sieburth et al. (31). After cultivation at 20°C, groups of synchronized, young adult WT and *pkc-2*$^{-/-}$ animals were incubated on lawns of *E. coli* OP50 at 17°C, 20°C, or 25°C for either 16 h or 20 min. Animals were then transferred to new plates equilibrated at the same temperatures. After a 5-min recovery period, the number of body bends observed in a 30-s interval was recorded for 10 animals in each group. Assays were replicated 3 times. Data are reported as body bends per minute. Mean values and standard errors of the means (SEM) were plotted.

Thermotaxis assays. *C. elegans* learns and remembers the cultivation temperature (T_c) when animals are incubated isothermally and fed high-quality food (22). Conditioned animals search for T_c when they encounter a temperature gradient. This beneficial learned behavior (thermotaxis) proceeds in two phases (47). First, animals randomly explore the gradient until they reach an elevated temperature ($>T_c$). They then migrate cryophilically toward the T_c by suppressing turning movements. Second, after locating the T_c, cryophilic migration ceases and animals track precisely along the T_c within the gradient. The AFD sensory neuron is the principal receiver, encoder, and transducer of ambient temperature changes in *C. elegans* (22, 25, 27). Signals generated in AFD are transmitted to the postsynaptic AIY interneuron and indirectly to secondary interneurons for processing and integration. Output signals from the interneurons regulate motor neurons that direct the animals toward the T_c.

Thermotaxis assays were performed as described by the Mori laboratory (72), using a radial temperature gradient of 17 to 25°C imposed across an agar surface in 10-cm petri plates. Animals were cultivated at 20°C (T_c), transferred to the 20°C region of assay plates, and allowed to migrate for 1 h. Movement was monitored and recorded by photographing the animal's tracks in the agar. Animals that move to a final destination at 17°C are designated cryophilic; worms that stably migrate to T_c exhibit normal isothermal tracking (plotted as animals at 20°C); animals that accumulate at 25°C are thermophilic; animals that move randomly over the gradient are designated atactic (plotted as AT). Fifty animals were used for each assay. In some instances, animals were incubated on cultivation plates containing 1.6 μM PMA for 2 h at 20°C before being transferred to assay plates.

Identification of neurons transcribing the *pkc-2* gene. A 1.5-kbp segment of DNA that terminates 13 bp upstream from the initiator ATG in exon 1A of the *pkc-2* gene (26) was inserted into the GFP expression vector pPD95.67 to create *pApkc-2*::GFP. A 3-kbp DNA fragment that terminates 9 bp upstream from the initiator ATG of exon 1B (26) was cloned into pPD95.67 to generate *pBpkc*-2::GFP. Recombinant plasmids were microinjected into WT *C. elegans*, and transgenic progeny were selected as described previously (69, 73). Neurons that have active *pkc-2* A and/or B promoters were located by monitoring GFP expression via microscopy. Neuron identities were assigned in accord with positional information provided in the *C. elegans* WormAtlas database (http://www.wormatlas.org), in conjunction with coexpression of neuron-specific red fluorescent protein (RFP) [oyIs44(*odr-1*::RFP)V, provided by Cori Bargmann (Rockefeller University) (74)] or a dye filling assay (75) in which a fluorescent carbocyanine compound is internalized by cilia of chemosensory neurons that contact the external environment (e.g., ASI, ASJ, and ADF). Fluorescence signals derived from transgenic animals were collected (1-μm sections) by using a Zeiss Imager Z1 microscope equipped with an ApoTome.

Expression of a *pkc-2* gene construct. The expression vector *pABCpkc*-2 was generated by digesting the cosmid E01H11 (26) with the restriction enzyme BsrGI to remove adjacent genes. A 40-kbp fragment that contains the *pkc-2* gene and endogenous A, B, and C promoter DNA was religated and cloned. *pABCpkc*-2 (1 ng/μl) and the *pBpkc-2*::GFP reporter gene were injected into *pkc-2*$^{-/-}$ animals, and transgenic progeny were selected as previously described (73). Subsequently, transgenic L4 nematodes were exposed to 3,000 rads of gamma irradiation from a ^{37}Cs source, and homogeneous populations of animals that express chromosomally integrated copies of *pABCpkc*-2 were established by standard methods (76).

Expression of PKC-2B cDNA (transgene) under regulation by endogenous promoters. PKC-2B and PKC-2A isoforms are generated by alternative splicing of *pkc-2* exon 13B or 13A (Fig. 1B), which encode distinct but homologous (~50% identical) C-terminal regions comprising 52 or 50 amino acids, respectively (26). Regulatory and kinase domains of PKCs 2B and 2A are identical. Given this minimal

difference and the desirability of eliminating unnecessary complexity, only cDNAs encoding mutant or WT PKC-2B were used in creating transgenic animals.

Classical restriction enzyme- and PCR-based genetic manipulation were used to prepare expression plasmids (derived from the pPD49.26 *C. elegans* vector) in which PKC-2B expression is controlled by the *pkc-2* A promoter (*pApkc-2*::PKC-2), B promoter (*pBpkc-2*::PKC-2), all three *pkc-2* promoters (*pABCpkc-2*::PKC-2), or the pan-neuronal *rgef-1* promoter (*prgef-1*::PKC-2). The vectors were injected into *pkc-2*$^{-/-}$ animals, and populations of animals expressing chromosomally integrated copies of each construct were produced as indicated above. Full details of the cloning procedures will be provided upon request.

Cell-specific expression of transgenes encoding mutant PKC-2B and UNC-18 proteins. Fragments of genomic promoter-enhancer DNA that precede the 5′ ends of the *inx-16* (830 bp), *gcy-8* (2,202 bp), and *col-19* (782 bp) genes were cloned into the *C. elegans* expression plasmid pPD49.26 (77). Regulatory elements in the *inx-16*, *gcy-8*, and *col-19* DNA fragments enable selective transcription of downstream transgenes (cDNAs) in intestinal epithelial cells, AFD neurons, and hypodermis, respectively (43–45). *inx-16* and *gcy-8* promoter DNAs were provided by Erik Jorgensen (Department of Biology, University of Utah) and Hannes Buelow (Department of Genetics, Albert Einstein College of Medicine), respectively. The *col-19* promoter DNA was amplified and cloned by Ya Fu in the Rubin laboratory. Full-length UNC-18 cDNA (clone 1308g1) was kindly provided by Y. Kohara (Genome Biology Laboratory, National Institute of Genetics, Mishima, Japan).

We performed site-directed mutagenesis to create dominant-negative (DN) and constitutively active (CA) PKC-2 variants and identify PKC-2 substrate sites in the UNC-18 protein. The PCR-based QuikChange mutagenesis kit (Agilent Technologies) was used according to the manufacturer's protocols. Replacement of Lys^{356} with Arg created DN PKC-2; replacement of Ala^{27} with Glu generated a CA variant of the kinase (see Results for details). The indicated mutations target catalytic and regulatory sites that are conserved in all DAG- and Ca^{2+}-regulated PKCs. Properties of DN and CA PKCs generated by this strategy have been thoroughly documented (39–42). Selected serines in the syntaxin binding loop of UNC-18 (Fig. 7 and associated text in Results) were replaced with alanine.

DN-PKC-2B and CA-PKC-2B cDNAs were cloned adjacent to the 3′ ends of *inx-16*, *gcy-8*, or *col-19* promoter sequence in recombinant pPD49.26 expression plasmids described above. Mutant UNC-18 cDNAs were cloned downstream from the *gcy-8* promoter in the pPD49.26 vector. Transgenic animals were generated by standard protocols as previously described (69, 73, 76).

Production and purification of GST–PKC-2B T651E. *In vitro* phosphorylation assays were used to identify PKC-2 substrate sites in the syntaxin binding loop of UNC-18. cDNA encoding a GST–PKC-2B fusion protein was cloned in the baculovirus transfer vector pVL1393. This enables the powerful polyhedron promoter to direct expression of the kinase in Sf9 insect cells. PKCs are made competent for activation by DAG and Ca^{2+} via sequential, posttranslational phosphorylations at the activation loop and then the turn motif, which is located near the C terminus (4, 78). However, after a conserved Thr in the turn motif is phosphorylated, activation loop phosphorylation becomes dispensable. The concentration of 3-phosphoinositide-dependent protein kinase 1 (PDK1), which catalyzes the critical phosphorylation of the activation loop, is low in Sf9 cells. Consequently, conserved Thr^{651} in the PKC-2B turn motif was mutated to phosphomimetic Glu to ensure that the recombinant kinase can be activated by Ca^{2+} and DAG-phosphatidylserine micelles *in vitro* (79).

Sf9 cells were grown in serum-free SF-900 II medium (Gibco) at 27°C. Cells were cotransfected with recombinant pVL1393 transfer plasmid containing GST–PKC-2B T651E cDNA and linearized baculoviral DNA (BaculoGold; BD Biosciences). After 72 h, recombinant baculovirus which contains the GST–PKC-2 T651E transgene was recovered in the medium. To obtain high-titer virus, the initial stock was amplified twice by infecting log-phase suspension cultures of Sf9 cells at a multiplicity of 0.1 and harvesting medium 5 days postinfection.

To express GST–PKC-2 T651E, log-phase Sf9 cells were infected with recombinant virus at a multiplicity of 5:1. After 72 h, medium was removed and cells were washed twice with phosphate-buffered saline (PBS). Further operations were performed at 0 to 4°C. Cells were lysed in 15 volumes of 10 mM sodium phosphate buffer, pH 7.4, containing 0.1 M NaCl, 1% Triton X-100, 1 mM dithiothreitol, 1× protease inhibitor cocktail I (Thermo Fisher), 1 μg/ml pepstatin, 10 μg/ml soybean trypsin inhibitor, and 10 mM benzamidine-HCl. The lysate was sonicated for 10 s and then clarified by centrifugation at 40,000 × *g* for 30 min. The supernatant solution was collected and GST–PKC-2B T651E was purified by affinity chromatography on glutathione (GSH)-Sepharose 4B beads, as previously reported (68).

Production and purification of GST–partial UNC-18 fusion proteins. Fragments of WT or mutated UNC-18 cDNA that encode amino acids 288 to 339 (Fig. 7B and associated text in Results) were amplified via PCR and cloned downstream from the GST gene in the isopropyl-1-thio-β-D-galactopyranoside-inducible bacterial expression plasmid pGex6P-1 (Promega). *E. coli* BL21 was transformed with a recombinant plasmid and incubated with 0.3 mM isopropyl-1-thio-β-D-galactopyranoside at 18°C for 16 h. Pelleted bacteria (1 g) were lysed by suspension in 5 ml BugBuster protein extraction reagent (70923; Novagen) containing 125 U of Benzonase nuclease (Santa Cruz Biotech), 10 kU rLysozyme (Novagen), and a cocktail of protease inhibitors (P8340; Sigma). The suspension was vigorously stirred for 1 h at 4°C. Subsequently, β-mercaptoethanol was added (final concentration, 1 mM) and the lysate was centrifuged at 44,000 × *g* for 20 min. WT or mutant GST–UNC-18 288-339 fusion proteins were isolated in the supernatant solution and then purified by affinity chromatography on GSH-Sepharose 4B beads as previously described (68).

Phosphorylation of WT and mutant UNC-18 syntaxin binding loops. WT or mutant GST–UNC-18 288-339 fusion protein (1 μg) was mixed with 20 mM HEPES-NaOH buffer, pH 7.5, containing 10 mM $MgCl_2$, 125 μM [γ-^{32}P]ATP, 0.4 mM $CaCl_2$, mixed DAG (8 ng/μl)-phosphatidylserine (20 ng/μl) micelles, 1

mM dithiothreitol, and 10 ng of highly purified GST–PKC-2B T651E in a volume of 20 μl. After incubation at 30°C for 30 min, SDS-PAGE loading buffer was added and samples were incubated at 95°C for 5 min. Proteins then were size fractionated by denaturing electrophoresis in a 12% polyacrylamide gel. The gel was stained with Coomassie blue, destained, and then dried. ^{32}P radioactivity incorporated into GST–UNC-18 fusion proteins was detected by exposing the dried gel to X-ray film. Bands were cut out and radioactivity was quantified by scintillation counting.

ACKNOWLEDGMENT

This work was supported by a grant from the NIH to C.S.R. (GM080615).

REFERENCES

1. Rhee SG. 2001. Regulation of phosphoinositide-specific phospholipase C. Annu Rev Biochem 70:281–312. https://doi.org/10.1146/annurev.biochem.70.1.281.
2. Mellor H, Parker PJ. 1998. The extended protein kinase C superfamily. Biochem J 332:281–292. https://doi.org/10.1042/bj3320281.
3. Newton AC. 2003. Regulation of the ABC kinases by phosphorylation: protein kinase C as a paradigm. Biochem J 370:361–371. https://doi.org/10.1042/bj20021626.
4. Steinberg SF. 2008. Structural basis of protein kinase C isoform function. Physiol Rev 88:1341–1378. https://doi.org/10.1152/physrev.00034.2007.
5. Rosse C, Linch M, Kermorgant S, Cameron AJ, Boeckeler K, Parker PJ. 2010. PKC and the control of localized signal dynamics. Nat Rev Mol Cell Biol 11:103–112. https://doi.org/10.1038/nrm2847.
6. Braz JC, Gregory K, Pathak A, Zhao W, Sahin B, Klevitsky R, Kimball TF, Lorenz JN, Nairn AC, Liggett SB, Bodi I, Wang S, Schwartz A, Lakatta EG, DePaoli-Roach AA, Robbins J, Hewett TE, Bibb JA, Westfall MV, Kranias EG, Molkentin JD. 2004. PKC-alpha regulates cardiac contractility and propensity toward heart failure. Nat Med 10:248–254. https://doi.org/10.1038/nm1000.
7. Antal CE, Hudson AM, Kang E, Zanca C, Wirth C, Stephenson NL, Trotter EW, Gallegos LL, Miller CJ, Furnari FB, Hunter T, Brognard J, Newton AC. 2015. Cancer-associated protein kinase C mutations reveal kinase's role as tumor suppressor. Cell 160:489–502. https://doi.org/10.1016/j.cell.2015.01.001.
8. Lim PS, Sutton CR, Rao S. 2015. Protein kinase C in the immune system: from signalling to chromatin regulation. Immunology 146:508–522. https://doi.org/10.1111/imm.12510.
9. Geraldes P, King GL. 2010. Activation of protein kinase C isoforms and its impact on diabetic complications. Circ Res 106:1319–1331. https://doi.org/10.1161/CIRCRESAHA.110.217117.
10. Sossin WS. 2007. Isoform specificity of protein kinase Cs in synaptic plasticity. Learn Mem 14:236–246. https://doi.org/10.1101/lm.469707.
11. Sun MK, Alkon DL. 2012. Activation of protein kinase C isozymes for the treatment of dementias. Adv Pharmacol 64:273–302. https://doi.org/10.1016/B978-0-12-394816-8.00008-8.
12. Sun MK, Alkon DL. 2014. The "memory kinases": roles of PKC isoforms in signal processing and memory formation. Prog Mol Biol Transl Sci 122:31–59. https://doi.org/10.1016/B978-0-12-420170-5.00002-7.
13. Fioravante D, Chu Y, de Jong AP, Leitges M, Kaeser PS, Regehr WG. 2014. Protein kinase C is a calcium sensor for presynaptic short-term plasticity. eLife 3:e03011.
14. Chu Y, Fioravante D, Leitges M, Regehr WG. 2014. Calcium-dependent PKC isoforms have specialized roles in short-term synaptic plasticity. Neuron 82:859–871. https://doi.org/10.1016/j.neuron.2014.04.003.
15. de Jong AP, Fioravante D. 2014. Translating neuronal activity at the synapse: presynaptic calcium sensors in short-term plasticity. Front Cell Neurosci 8:356. https://doi.org/10.3389/fncel.2014.00356.
16. Chen DH, Brkanac Z, Verlinde CL, Tan XJ, Bylenok L, Nochlin D, Matsushita M, Lipe H, Wolff J, Fernandez M, Cimino PJ, Bird TD, Raskind WH. 2003. Missense mutations in the regulatory domain of PKC gamma: a new mechanism for dominant nonepisodic cerebellar ataxia. Am J Hum Genet 72:839–849. https://doi.org/10.1086/373883.
17. Verbeek DS, Goedhart J, Bruinsma L, Sinke RJ, Reits EA. 2008. PKC gamma mutations in spinocerebellar ataxia type 14 affect C1 domain accessibility and kinase activity leading to aberrant MAPK signaling. J Cell Sci 121:2339–2349. https://doi.org/10.1242/jcs.027698.
18. Alfonso SI, Callender JA, Hooli B, Antal CE, Mullin K, Sherman MA, Lesne SE, Leitges M, Newton AC, Tanzi RE, Malinow R. 2016. Gain-of-function mutations in protein kinase Calpha (PKCalpha) may promote synaptic defects in Alzheimer's disease. Sci Signal 9:ra47. https://doi.org/10.1126/scisignal.aaf6209.
19. Hsieh H, Boehm J, Sato C, Iwatsubo T, Tomita T, Sisodia S, Malinow R. 2006. AMPAR removal underlies Abeta-induced synaptic depression and dendritic spine loss. Neuron 52:831–843. https://doi.org/10.1016/j.neuron.2006.10.035.
20. Weeber EJ, Atkins CM, Selcher JC, Varga AW, Mirnikjoo B, Paylor R, Leitges M, Sweatt JD. 2000. A role for the beta isoform of protein kinase C in fear conditioning. J Neurosci 20:5906–5914.
21. Zhang GR, Liu M, Cao H, Kong L, Wang X, O'Brien JA, Wu SC, Cook RG, Geller AI. 2009. Improved spatial learning in aged rats by genetic activation of protein kinase C in small groups of hippocampal neurons. Hippocampus 19:413–423. https://doi.org/10.1002/hipo.20506.
22. Mori I, Sasakura H, Kuhara A. 2007. Worm thermotaxis: a model system for analyzing thermosensation and neural plasticity. Curr Opin Neurobiol 17:712–719. https://doi.org/10.1016/j.conb.2007.11.010.
23. Garrity PA, Goodman MB, Samuel AD, Sengupta P. 2010. Running hot and cold: behavioral strategies, neural circuits, and the molecular machinery for thermotaxis in C. elegans and Drosophila. Genes Dev 24:2365–2382. https://doi.org/10.1101/gad.1953710.
24. Sasakura H, Mori I. 2013. Behavioral plasticity, learning, and memory in C. elegans. Curr Opin Neurobiol 23:92–99. https://doi.org/10.1016/j.conb.2012.09.005.
25. Aoki I, Mori I. 2015. Molecular biology of thermosensory transduction in C. elegans. Curr Opin Neurobiol 34:117–124. https://doi.org/10.1016/j.conb.2015.03.011.
26. Islas-Trejo A, Land M, Tcherepanova I, Freedman JH, Rubin CS. 1997. Structure and expression of the Caenorhabditis elegans protein kinase C2 gene. Origins and regulated expression of a family of Ca2+-activated protein kinase C isoforms. J Biol Chem 272:6629–6640.
27. Tsukada Y, Yamao M, Naoki H, Shimowada T, Ohnishi N, Kuhara A, Ishii S, Mori I. 2016. Reconstruction of spatial thermal gradient encoded in thermosensory neuron AFD in Caenorhabditis elegans. J Neurosci 36:2571–2581. https://doi.org/10.1523/JNEUROSCI.2837-15.2016.
28. Bargmann CI, Hartwieg E, Horvitz HR. 1993. Odorant-selective genes and neurons mediate olfaction in C. elegans. Cell 74:515–527. https://doi.org/10.1016/0092-8674(93)80053-H.
29. Biron D, Wasserman S, Thomas JH, Samuel AD, Sengupta P. 2008. An olfactory neuron responds stochastically to temperature and modulates Caenorhabditis elegans thermotactic behavior. Proc Natl Acad Sci U S A 105:11002–11007. https://doi.org/10.1073/pnas.0805004105.
30. Kuhara A, Okumura M, Kimata T, Tanizawa Y, Takano R, Kimura KD, Inada H, Matsumoto K, Mori I. 2008. Temperature sensing by an olfactory neuron in a circuit controlling behavior of C. elegans. Science 320:803–807. https://doi.org/10.1126/science.1148922.
31. Sieburth D, Madison JM, Kaplan JM. 2007. PKC-1 regulates secretion of neuropeptides. Nat Neurosci 10:49–57. https://doi.org/10.1038/nn1810.
32. Chen L, Fu Y, Ren M, Xiao B, Rubin CS. 2011. A RasGRP, C elegans RGEF-1b, couples external stimuli to behavior by activating LET-60 (Ras) in sensory neurons. Neuron 70:51–65. https://doi.org/10.1016/j.neuron.2011.02.039.
33. Coburn CM, Bargmann CI. 1996. A putative cyclic nucleotide-gated channel is required for sensory development and function in C. elegans. Neuron 17:695–706. https://doi.org/10.1016/S0896-6273(00)80201-9.
34. Komatsu H, Mori I, Rhee JS, Akaike N, Ohshima Y. 1996. Mutations in a cyclic nucleotide-gated channel lead to abnormal thermosensation and chemosensation in C. elegans. Neuron 17:707–718. https://doi.org/10.1016/S0896-6273(00)80202-0.
35. Komatsu H, Jin YH, L'Etoile N, Mori I, Bargmann CI, Akaike N, Ohshima Y. 1999. Functional reconstitution of a heteromeric cyclic nucleotide-gated

channel of Caenorhabditis elegans in cultured cells. Brain Res 821:160–168. https://doi.org/10.1016/S0006-8993(99)01111-7.
36. Gray JM, Karow DS, Lu H, Chang AJ, Chang JS, Ellis RE, Marletta MA, Bargmann CI. 2004. Oxygen sensation and social feeding mediated by a C. elegans guanylate cyclase homologue. Nature 430:317–322. https://doi.org/10.1038/nature02714.
37. Xiao R, Zhang B, Dong Y, Gong J, Xu T, Liu J, Xu XZ. 2013. A genetic program promotes C. elegans longevity at cold temperatures via a thermosensitive TRP channel. Cell 152:806–817. https://doi.org/10.1016/j.cell.2013.01.020.
38. Takeishi A, Yu YV, Hapiak VM, Bell HW, O'Leary T, Sengupta P. 2016. Receptor-type guanylyl cyclases confer thermosensory responses in C. elegans. Neuron 90:235–244. https://doi.org/10.1016/j.neuron.2016.03.002.
39. Garcia-Paramio P, Cabrerizo Y, Bornancin F, Parker PJ. 1998. The broad specificity of dominant inhibitory protein kinase C mutants infers a common step in phosphorylation. Biochem J 333:631–636. https://doi.org/10.1042/bj3330631.
40. Genot EM, Parker PJ, Cantrell DA. 1995. Analysis of the role of protein kinase C-alpha, -epsilon, and -zeta in T cell activation. J Biol Chem 270:9833–9839. https://doi.org/10.1074/jbc.270.17.9833.
41. Pears CJ, Kour G, House C, Kemp BE, Parker PJ. 1990. Mutagenesis of the pseudosubstrate site of protein kinase C leads to activation. Eur J Biochem 194:89–94. https://doi.org/10.1111/j.1432-1033.1990.tb19431.x.
42. Soh JW, Lee EH, Prywes R, Weinstein IB. 1999. Novel roles of specific isoforms of protein kinase C in activation of the c-fos serum response element. Mol Cell Biol 19:1313–1324. https://doi.org/10.1128/MCB.19.2.1313.
43. Yu S, Avery L, Baude E, Garbers DL. 1997. Guanylyl cyclase expression in specific sensory neurons: a new family of chemosensory receptors. Proc Natl Acad Sci U S A 94:3384–3387. https://doi.org/10.1073/pnas.94.7.3384.
44. Peters MA, Teramoto T, White JQ, Iwasaki K, Jorgensen EM. 2007. A calcium wave mediated by gap junctions coordinates a rhythmic behavior in C. elegans. Curr Biol 17:1601–1608. https://doi.org/10.1016/j.cub.2007.08.031.
45. Liu Z, Kirch S, Ambros V. 1995. The Caenorhabditis elegans heterochronic gene pathway controls stage-specific transcription of collagen genes. Development 121:2471–2478.
46. Husson SJ, Clynen E, Baggerman G, Janssen T, Schoofs L. 2006. Defective processing of neuropeptide precursors in Caenorhabditis elegans lacking proprotein convertase 2 (KPC-2/EGL-3): mutant analysis by mass spectrometry. J Neurochem 98:1999–2012. https://doi.org/10.1111/j.1471-4159.2006.04014.x.
47. Luo L, Cook N, Venkatachalam V, Martinez-Velazquez LA, Zhang X, Calvo AC, Hawk J, MacInnis BL, Frank M, Ng JH, Klein M, Gershow M, Hammarlund M, Goodman MB, Colon-Ramos DA, Zhang Y, Samuel AD. 2014. Bidirectional thermotaxis in Caenorhabditis elegans is mediated by distinct sensorimotor strategies driven by the AFD thermosensory neurons. Proc Natl Acad Sci U S A 111:2776–2781. https://doi.org/10.1073/pnas.1315205111.
48. Sudhof TC. 2014. The molecular machinery of neurotransmitter release (Nobel lecture). Angew Chem Int 53:12696–12717. https://doi.org/10.1002/anie.201406359.
49. Rizo J, Xu J. 2015. The synaptic vesicle release machinery. Annu Rev Biophys 44:339–367. https://doi.org/10.1146/annurev-biophys-060414-034057.
50. Sassa T, Harada S, Ogawa H, Rand JB, Maruyama IN, Hosono R. 1999. Regulation of the UNC-18-Caenorhabditis elegans syntaxin complex by UNC-13. J Neurosci 19:4772–4777.
51. Johnson JR, Ferdek P, Lian LY, Barclay JW, Burgoyne RD, Morgan A. 2009. Binding of UNC-18 to the N-terminus of syntaxin is essential for neurotransmission in Caenorhabditis elegans. Biochem J 418:73–80. https://doi.org/10.1042/BJ20081956.
52. Fioravante D, Chu Y, Myoga MH, Leitges M, Regehr WG. 2011. Calcium-dependent isoforms of protein kinase C mediate posttetanic potentiation at the calyx of Held. Neuron 70:1005–1019. https://doi.org/10.1016/j.neuron.2011.04.019.
53. Fujita Y, Sasaki T, Fukui K, Kotani H, Kimura T, Hata Y, Sudhof TC, Scheller RH, Takai Y. 1996. Phosphorylation of Munc-18/n-Sec1/rbSec1 by protein kinase C: its implication in regulating the interaction of Munc-18/n-Sec1/rbSec1 with syntaxin. J Biol Chem 271:7265–7268. https://doi.org/10.1074/jbc.271.13.7265.
54. Wierda KD, Toonen RF, de Wit H, Brussaard AB, Verhage M. 2007. Interdependence of PKC-dependent and PKC-independent pathways for presynaptic plasticity. Neuron 54:275–290. https://doi.org/10.1016/j.neuron.2007.04.001.
55. Edwards MR, Johnson JR, Rankin K, Jenkins RE, Maguire C, Morgan A, Burgoyne RD, Barclay JW. 2012. PKC-2 phosphorylation of UNC-18 Ser322 in AFD neurons regulates temperature dependency of locomotion. J Neurosci 32:7042–7051. https://doi.org/10.1523/JNEUROSCI.4029-11.2012.
56. Genc O, Kochubey O, Toonen RF, Verhage M, Schneggenburger R. 2014. Munc18-1 is a dynamically regulated PKC target during short-term enhancement of transmitter release. eLife 3:e01715.
57. Barclay JW, Craig TJ, Fisher RJ, Ciufo LF, Evans GJ, Morgan A, Burgoyne RD. 2003. Phosphorylation of Munc18 by protein kinase C regulates the kinetics of exocytosis. J Biol Chem 278:10538–10545. https://doi.org/10.1074/jbc.M211114200.
58. Cijsouw T, Weber JP, Broeke JH, Broek JA, Schut D, Kroon T, Saarloos I, Verhage M, Toonen RF. 2014. Munc18-1 redistributes in nerve terminals in an activity- and PKC-dependent manner. J Cell Biol 204:759–775. https://doi.org/10.1083/jcb.201308026.
59. Yu YV, Bell HW, Glauser DA, Van Hooser SD, Goodman MB, Sengupta P. 2014. CaMKI-dependent regulation of sensory gene expression mediates experience-dependent plasticity in the operating range of a thermosensory neuron. Neuron 84:919–926. https://doi.org/10.1016/j.neuron.2014.10.046.
60. Kuhara A, Ohnishi N, Shimowada T, Mori I. 2011. Neural coding in a single sensory neuron controlling opposite seeking behaviours in Caenorhabditis elegans. Nat Commun 2:355. https://doi.org/10.1038/ncomms1352.
61. Hu SH, Christie MP, Saez NJ, Latham CF, Jarrott R, Lua LH, Collins BM, Martin JL. 2011. Possible roles for Munc18-1 domain 3a and Syntaxin1 N-peptide and C-terminal anchor in SNARE complex formation. Proc Natl Acad Sci U S A 108:1040–1045. https://doi.org/10.1073/pnas.0914906108.
62. Parisotto D, Pfau M, Scheutzow A, Wild K, Mayer MP, Malsam J, Sinning I, Sollner TH. 2014. An extended helical conformation in domain 3a of Munc18-1 provides a template for SNARE (soluble N-ethylmaleimide-sensitive factor attachment protein receptor) complex assembly. J Biol Chem 289:9639–9650. https://doi.org/10.1074/jbc.M113.514273.
63. Munch AS, Kedar GH, van Weering JR, Vazquez-Sanchez S, He E, Andre T, Braun T, Sollner TH, Verhage M, Sorensen JB. 2016. Extension of helix 12 in Munc18-1 induces vesicle priming. J Neurosci 36:6881–6891. https://doi.org/10.1523/JNEUROSCI.0007-16.2016.
64. Chen YC, Chen HJ, Tseng WC, Hsu JM, Huang TT, Chen CH, Pan CL. 2016. A C. elegans thermosensory circuit regulates longevity through crh-1/CREB-dependent flp-6 neuropeptide signaling. Dev Cell 39:209–223. https://doi.org/10.1016/j.devcel.2016.08.021.
65. Okochi Y, Kimura KD, Ohta A, Mori I. 2005. Diverse regulation of sensory signaling by C. elegans nPKC-epsilon/eta TTX-4. EMBO J 24:2127–2137. https://doi.org/10.1038/sj.emboj.7600697.
66. Fu Y, Ren M, Feng H, Chen L, Altun ZF, Rubin CS. 2009. Neuronal and intestinal protein kinase d isoforms mediate Na+ (salt taste)-induced learning. Sci Signal 2:ra42. https://doi.org/10.1126/scisignal.2000224.
67. Sugi T, Nishida Y, Mori I. 2011. Regulation of behavioral plasticity by systemic temperature signaling in Caenorhabditis elegans. Nat Neurosci 14:984–992. https://doi.org/10.1038/nn.2854.
68. Land M, Islas-Trejo A, Freedman JH, Rubin CS. 1994. Structure and expression of a novel, neuronal protein kinase C (PKC1B) from Caenorhabditis elegans. PKC1B is expressed selectively in neurons that receive, transmit, and process environmental signals. J Biol Chem 269:9234–9244.
69. Feng H, Ren M, Wu SL, Hall DH, Rubin CS. 2006. Characterization of a novel protein kinase D: Caenorhabditis elegans DKF-1 is activated by translocation-phosphorylation and regulates movement and growth in vivo. J Biol Chem 281:17801–17814. https://doi.org/10.1074/jbc.M511899200.
70. Ndubuka C, Li Y, Rubin CS. 1993. Expression of a kinase anchor protein 75 depletes type II cAMP-dependent protein kinases from the cytoplasm and sequesters the kinases in a particulate pool. J Biol Chem 268:7621–7624.
71. Hirsch AH, Glantz SB, Li Y, You Y, Rubin CS. 1992. Cloning and expression of an intron-less gene for AKAP 75, an anchor protein for the regulatory subunit of cAMP-dependent protein kinase II beta. J Biol Chem 267:2131–2134.
72. Mohri A, Kodama E, Kimura KD, Koike M, Mizuno T, Mori I. 2005. Genetic control of temperature preference in the nematode Caenorhabditis elegans. Genetics 169:1437–1450. https://doi.org/10.1534/genetics.104.036111.

73. Freedman JH, Slice LW, Dixon D, Fire A, Rubin CS. 1993. The novel metallothionein genes of Caenorhabditis elegans. Structural organization and inducible, cell-specific expression. J Biol Chem 268:2554–2564.
74. Sagasti A, Hisamoto N, Hyodo J, Tanaka-Hino M, Matsumoto K, Bargmann CI. 2001. The CaMKII UNC-43 activates the MAPKKK NSY-1 to execute a lateral signaling decision required for asymmetric olfactory neuron fates. Cell 105:221–232. https://doi.org/10.1016/S0092-8674(01)00313-0.
75. Hedgecock EM, Culotti JG, Thomson JN, Perkins LA. 1985. Axonal guidance mutants of Caenorhabditis elegans identified by filling sensory neurons with fluorescein dyes. Dev Biol 111:158–170. https://doi.org/10.1016/0012-1606(85)90443-9.
76. Mello CC, Kramer JM, Stinchcomb D, Ambros V. 1991. Efficient gene transfer in C. elegans: extrachromosomal maintenance and integration of transforming sequences. EMBO J 10:3959–3970.
77. Fire A, Harrison SW, Dixon D. 1990. A modular set of lacZ fusion vectors for studying gene expression in Caenorhabditis elegans. Gene 93:189–198. https://doi.org/10.1016/0378-1119(90)90224-F.
78. Newton AC. 2010. Protein kinase C: poised to signal. Am J Physiol Endocrinol Metab 298:E395–E402. https://doi.org/10.1152/ajpendo.00477.2009.
79. Edwards AS, Faux MC, Scott JD, Newton AC. 1999. Carboxyl-terminal phosphorylation regulates the function and subcellular localization of protein kinase C betaII. J Biol Chem 274:6461–6468. https://doi.org/10.1074/jbc.274.10.6461.
80. Rossi EA, Li Z, Feng H, Rubin CS. 1999. Characterization of the targeting, binding, and phosphorylation site domains of an A kinase anchor protein and a myristoylated alanine-rich C kinase substrate-like analog that are encoded by a single gene. J Biol Chem 274:27201–27210. https://doi.org/10.1074/jbc.274.38.27201.